GE Energy

David H. Hinds
Manager, ESBWR

PO Box 780 M/C L60
Wilmington, NC 28402-0780
USA

T 910 675 6363
F 910 362 6363
david.hinds@ge.com

MFN 06-040

Docket No. 52-010

February 14, 2006

U.S. Nuclear Regulatory Commission
Document Control Desk
Washington, D.C. 20555-0001

Subject: **Additional Information Related to ESBWR Fission Product Removal**

In the Reference 1 letter, GE indicated that supporting information related to the ESBWR fission product removal evaluation model would be provided under separate cover. Enclosure 1 contains this additional supporting information:

- ECN Nuclear Energy Report No. ECN-CX-96-124, *Fission Product Retention Within the ESBWR Containment,* December 1996

If you have any questions about the information provided here, please let me know.

Sincerely,

/ LA Upton for

David H. Hinds
Manager, ESBWR

Reference:

1. MFN 06-032, Letter from David H. Hinds to U.S. Nuclear Regulatory Commission, *Framework and Schedule for GE Licensing Topical Report Related to ESBWR Fission Product Removal,* January 25, 2006

D068

Enclosure:

1. MFN 06-040 – ECN Nuclear Energy Report No. ECN-CX-96-124, "Fission Product Retention Within the ESBWR Containment," December 1996

cc: WD Beckner USNRC (w/o enclosures)
AE Cubbage USNRC (with enclosures)
LA Dudes USNRC (w/o enclosures)
GB Stramback GE/San Jose (with enclosures)
eDRF 0000-0031-5955

ENCLOSURE 1

MFN 06-040

ECN Nuclear Energy Report No. ECN-CX-96-124,

"Fission Product Retention Within the ESBWR Containment,"

December 1996

DECEMBER 1996 ECN-CX-96-124

FISSION PRODUCT RETENTION WITHIN THE ESBWR CONTAINMENT

A. WOUDSTRA

Revises		
A	Preliminary Issue	December 13, 1996
1	Final Issue	December 31, 1996

Made by A. Woudstra	**Approved by** S. Spoelstra	ECN Nuclear Energy Safety & Reliability Engineering
Checked by N.B. Siccama	**Issues** P.M. Stoop	

This report has been prepared within the framework of the PINK-LWR project 71153 as part of the ECN contribution to the ESBWR project.

Abstract

This document presents the results of an analysis performed with the MELCOR computer code to determine the natural retention of fission products within the containment of the ESBWR during the first 24 hours. The accident considered in this report concerns a design-basis accident scenario in which the containment remains intact but leaks according to the Technical Specifications. The design leak rate of the containment is 0.5 vol.%/day at a design pressure of 0.483 MPA.

The masses of steam and hydrogen being released from the reactor pressure vessel (RPV) to the containment have been calculated by GE with the MAAP code and have been used as input for the MELCOR analysis. The source term from the RPV into the containment is based on the gap release and the early in-vessel release, which are taken from NUREG-1465.

In the 24-hr time period, a fraction of $5.4 * 10^{-4}$ of the noble gases in the containment leaks to the reactor building (RB). With respect to the aerosols, the fraction of aerosols in the containment that leaks to the RB is almost independent of the aerosol species and equals $2.7*10^{-4}$ after 24 hr.

Distribution:

GE : 1-5

ECN : 6-25

Table of Contents

1. Introduction

Based on the SBWR (Simplified Boiling Water Reactor) concept an ESBWR (European Simplified Boiling Water Reactor) is developed by GE (General Electric) for the European market. The ESBWR is a natural circulation 1190 MWe design that utilizes simplified design and passive systems to enhance the overall safety of the design. A safety barrier like a "safety envelope" will be omitted in the ESBWR design to make the design competitive in economic respect.

In order to assess the risk to public health and safety resulting from operation of a nuclear power plant, the regulatory body requires that the radiological consequences of potential releases of fission products to the environment be evaluated.

For licensing purposes, the design of the containment and engineered safety features are evaluated by radiological analysis of postulated accident scenarios (design basis accidents) which results in the release of fission products. For instance, a design basis accident LOCA release uses a postulated "in-containment accident source term" which is normally a function of time and will involve consideration of fission products being released from the core into the containment as well as removal of fission products by plant features intended to do so (e.g. spray systems) or by natural removal processes. Moreover, it is assumed that the containment stays intact but leaks to the RB. Possibly, the PCCS (Passive Containment Cooling System) functions as a passive aerosol filter. A significant fraction of the generated aerosols is passed along the PCCS heat exchangers which may be able to remove most of the aerosols.

This document presents the calculational results obtained from a MELCOR analysis which has been performed to determine the magnitude of the natural retention processes within the containment of the ESBWR. The MELCOR code models describing the dominant physical phenomena for fission product retention analyses are described in chapter 2. The MELCOR input model for this problem is presented in chapter 3. Chapter 4 describes the analysis results. Finally, the conclusions of the fission products retention analysis are given in chapter 5.

2. MELCOR Computer Code

Introduction

MELCOR is a fully integrated, engineering-level computer code that models the progression of severe accidents in Light Water Reactor nuclear power plants [1]. MELCOR is being developed at Sandia National Laboratories for the U.S. Nuclear Regulatory Commission (US-NRC) as a second-generation plant risk assessment tool. The spectrum of severe accident phenomena, including reactor coolant system and containment thermal-hydraulic response, core heat-up, degradation and relocation, and fission product release and transport, are treated in MELCOR in a unified framework for both boiling water reactors and pressurized water reactors. MELCOR has especially been designed to facilitate sensitivity and uncertainty analyses. The targeted applications envisioned by the NRC for MELCOR are BWR and PWR Probabilistic Risk Assessment (PRA) studies, audit reviews of the Individual Plant Examination (IPE) submittals, studies to develop insights into phenomena and hardware performance, and accident management studies.

MELCOR has been under development since 1982. The latest version is MELCOR 1.8.3, released in July 1994. The calculations in this report have been performed with this latest version which is installed on an IBM RS6000 workstation.

Thermal-hydraulic modeling

Thermal-hydraulic behaviour is modeled in MELCOR in terms of control volumes and flow paths. All hydrodynamic material (and its energy) resides in control volumes. Hydrodynamic material includes the coolant and noncondensible gases. These materials are assumed to separate under influence of gravity within a control volume to form a 'pool' beneath an 'atmosphere'. Each control volume is characterized by one single pressure and two temperatures, one temperature for the pool and one for the atmosphere.

The control volumes are connected by flow paths through which the hydrodynamic materials may move without residence time, driven by a momentum equation. Based on the elevations of the pool surfaces in the connected control volumes relative to the junctions with the flow paths, both pool and atmosphere may pass through each flow path. Appropriate hydrostatic head terms are included in the momentum equation for the flow paths, allowing calculation of natural circulation.

Heat structure modeling

A heat structure is an intact, solid structure which is represented by one-dimensional heat conduction with specified boundary conditions at each of its two boundary surfaces. The modeling capabilities of heat structures are general and can include pressure vessel internals and walls, containment structures and walls, fuel rods with nuclear or electrical heating, steam generator tubes, piping walls, etc. A heat structure may have a rectangular, cylindrical, spherical, or hemispherical geometry. The number of mesh intervals within a heat structure is specified by user input and may be nonuniform, i.e. the distance between temperature nodes need not be the same. Each mesh interval may contain a different material.

Steam condensation

Mass transfer between a heat structure surface and the boundary volume atmosphere is modeled using correlations for calculating the mass flux. Models include condensation in a pure steam environment, condensation and evaporation in the presence of noncondensibles, and flashing in any environment. Liquid films on heat structure surfaces are also modeled so that condensate transferred from the boundary volume atmosphere and liquid deposited by other packages can be treated. Mass transfer affects the temperature distribution within a heat structure by its energy flux at the surface. When mass transfer occurs at a structure surface, an equation for the surface temperature of the resulting liquid film including the energy flux due to mass transfer is included in the set of conduction (temperature) equations for the structure.

Film-tracking model

If a heat structure is part of a film-tracking network, then the condensate film thickness will be determined dynamically as a function of the film flow rate. The drainage from the surface will be partitioned between the boundary volume pool, the boundary volume fog, and the surfaces of other heat structures in the user-specified network. In case the film-tracking model is used, the aerosols are assumed to stick to the wall. If the film-tracking model is not used the user can select if the aerosols flow downwards with the water film on the walls, stick to the walls, or any option in between.

MELCOR Fission Product behavior modeling

MELCOR calculates both the release and transport behavior of fission products. It tracks the masses of fission products by material classes. Each material class represents a group of one or more elements with similar physical properties. Each class has its own set of values of importance, such as release coefficients and vapor pressure. Table 2.1 lists the 15 default classes used in MELCOR. Class 16 in this table has been added for ESBWR purposes to model CsI.

The aerosol dynamics portion of the MELCOR code is based on the MAEROS computer program [2], except for the condensation model. MAEROS is a multicomponent aerosol dynamics code which evaluates the dynamic particle size distribution of each component. This size distribution is described by the mass in each section, or size bin, Both agglomeration and deposition effects are included in MELCOR. Agglomeration of aerosols by Brownian motion, gravity, and turbulence is accounted for. The deposition processes which are modeled in MELCOR are: gravity, Brownian diffusion, thermophoresis, and diffusiophoresis.

Hygroscopic effects and the Kelvin effect which may play an important role for aerosol behavior in saturated or nearly saturated conditions, are not modeled in the MELCOR code. Excluding hygroscopic effects is a conservative approximation for the analyses described in this report since bulk condensation onto aerosols will result in larger aerosols which settle out faster. In addition, the Kelvin effect only becomes important for very small particles which do not occur in these analyses.

Aerosols and fission product vapors can deposit directly on surfaces such as heat structures and water pools. In addition, aerosols can agglomerate and settle. The aerosols deposited on the various surfaces cannot currently be resuspended. If a water film drains from a heat structure to the pool in the associated volume, fission products deposited on that surface are relocated with the water. This relocation is proportional to the fraction of the film that is drained.

Aerosols and fission product vapors are transported between control volumes by bulk fluid flow of the atmosphere and the pool, assuming zero slip. In addition, aerosols may "settle" from a volume to a lower situated volume in the absence of bulk flow.

MAEROS Code

Dynamic particle size distribution of each component

- Agglomeration
  - Brownian motion
  - Gravity
  - Turbulence
- Deposition
  - Brownian diffusion
  - Gravity
  - Thermophoresis
  - diffusiophoresis

(Size distribution described by mass in each section, or site bin.)

,

/

Table 2.1 MELCOR fission product classes

Nr	Class name	Representative	Member elements
I	Noble gases	Xe	He, Ne, Ar, Kr, Xe, Rn, H, N
2	ALkali metals	Cs	Li, Na, K, Rb, Cs, Fr, Cu
3	Alkaline Earths	Ba	Be, Mg, Ca, Sr, Ba, Ra, Es, Fm
4	Halogens	I	F, Cl, Br, I, At
5	Chalcogens	Te	O, S, Se, Te, Po
6	Platinoids	Ru	Ru, Rh, Pd, Re, Os, Ir, Pt, Au, Ni
7	Early Transition Elements	Mo	V, Cr, Fe, Co, Mn, Nb, Mo, Tc, Ta, W
8	Tetravalent	Ce	Ti, Zr, Hf, Ce, Th, Pa, Np, Pu, C
9	Trivalents	La	A1, Sc, Y, La, Ac, Pr, Nd, Pm, Sm, Eu, Gd, Tb, Dy, Ho, Er, Tm, Yb, Lu, Am, Cm, Bk, Cf
10	Uranium	U	U
11	More Volatile Main Group	Cd	Cd, Hg, Zn, As, Sb, Pb, T1, Bi
12	Less Volatile Main Group	Sn	Ga, Ge, In, Sn, Ag
13	Boron	B	B, Si, P
14	Water	H_2O	H_2O
15	Concrete	---	---
16	Cesium Iodine	CsI	CsI

3. MELCOR Input Model

In this chapter, the MELCOR input model for the containment analysis is described.

3.1 MELCOR containment input model

The MELCOR nodalization scheme is obtained by a subdivision of the containment into 15 control volumes and 21 flow paths. Some additional volumes have been added to represent the RB and the Isolation Condenser (IC) pool, in which the Passive Containment Cooling System (PCCS) is located. The resulting nodalization scheme is depicted in Figure 3.1. The total volume of the containmnent equals 15500 m^3. The subdivision of the containment volumes is given in Table 3.1.

Heat transfer between control volumes and between control volumes and internal structures is taken into account by a total number of 30 heat structures.

Fission product behaviour, including transport through the containment volumes, and deposition on the various structures and pools is taken into account. Pool scrubbing occurs between the vents and the wetwell and between the PCCS and the wetwell.

The transport of fission products between the containment and the RB occurs because the containment leaks due to the pressure increase during the accident. Gases and aerosols leak from the upper drywell volume along penetrations into the RB. In the analyses, the leak rate through the penetrations is based on the design leak rate, which is 0.5 vol. %/day at a pressure of 0.483 MPa. Based on a containment free volume of 16357 m^3 this equals a volumetric flow rate of $9.466*10^{-4}$ m^3/s. Assuming 100 % steam this corresponds to a mass flow of $2.444*10^{-3}$ kg/s steam leaking from the containment. To model the leak flow from the containment at the actual pressure, a leak area of $3.28 * 10^{-6}$ m^2 is modeled in the upper drywell region.

The release of the fission products from the upper drywell to the RB is calculated under the assumption that the upper drywell atmosphere including fission products is ideally mixed.

The condensation model in MELCOR allows steam to condense on all existing aerosols. In fact, this is the more realistic condensation model. However, in case of evaporation, the particle size is not modeled correctly and decreases to very low values. For this reason, in the present containment analysis, steam is only allowed to condense onto existing water aerosols and not onto fission product aerosols.

Table 3.2 shows the initial conditions inside the ESBWR containment compartments, the IC-pool, and the RB [7].

3.2 Boundary conditions

The basis for the analyses is a design-basis loss-of-coolant accident. All emergency core cooling systems are assumed to fail initially. However, 2.5 hours after the water level drops below the top of the active fuel, GDCS (Gravity Driven Core Cooling System) is initiated and the molten core material is "saved" in-vessel. The GDCS starts draining at about 3.5 hours after the start of the accident with a mass flow rate of 500 ton/hr.

The mass flow rates of steam and hydrogen as well as the enthalpies and temperatures of these gases have been obtained from a MAAP analysis data file [3]. This MAAP data concern an analysis for a 670 MWe SBWR. Therefore the MAAP mass flows are multiplied by a factor of 1.8 to represent the break input data for the ESBWR design. This factor equals the ESBWR/SBWR power ratio. The break input data are shown in Figure 3.2-3.5.

The core inventory of fission products for the 670 MWe SBWR is given in [4]. This core inventory also is multiplied by a factor of 1.8 to represent the core inventory for the ESBWR design. The ESBWR core inventory is given in Table 3.3.

The fission product release from the RPV into the containment stems from NUREG-1465 [5]. Two successive periods are distinguished for the fission product release:

1. Gap release (0.5 hr)
2. Early in-vessel release (1.5 hr)

The release of fission products during the "gap release" starts some time after the cladding oxidation. The cladding fails about 10 minutes after 1 kg of hydrogen has been produced [6]. According to [3] it takes 4935 seconds to produce 1 kg of hydrogen. So the start of the "gap release" begins at t = 4935 + 10 * 60 = 5535 seconds.

At the end of the early in-vessel release period, which is 3.5 hours after the start of the accident, the fission products release stops. Since the core melt is saved in-vessel, and the bottom head of the RPV does not fail, the "late in-vessel release" and the "ex-vessel release", as mentioned in [5], do not occur. The source term fractions for the two release periods are given in Table 3.4.

All fission products, except for the noble gases, are assumed to be released in particulate form. The initial particle size distribution of these released aerosols is characterized by an aerodynamic mass median diameter of 1.0 μm and a geometric standard deviation of 1.6. These values are considered to be representative for the release from the RPV.

Table 3.1 Volumes within the ESBWR containment

Node	Description	Volume in [m^3]
201	Lower drywell	1305.0
202	Central drywell	703.0
203	Upper drywell	3395.0
204	Vents	125.0
205	Wetwell	7820.0
206	GDCS	1425.0
207	Annulus	377.0
208	Head	315.0
209	PCCS water box	12.7
210	PCCS tubes	10.0
211	PCCS steam box	11.9
-	RPV	857.0
	Total	16357

Table 3.2 Initial conditions

				Fraction		
Location	Pressure [MPa]	Temperature [K]	Relative humidity [%]	N_2 [-]	O_2 [-]	Pool mass [1-3 kg]
Drywell	0.10983	330.35	20	0.97	0.03	0
Wetwell	0.10983	316.45	100	0.97	0.03	3570
Vents	0.10983	316.45	100	0.97	0.03	53
GDCS	0.10983	330.35	100	0.97	0.03	1296
IC	0.10130	300.0	100	0.80	0.20	4740
Reactor building	0.10130	300.0	100	0.80	0.20	495

Table 3.3 Initial ESBWR core inventory

MELCOR class	Fission product	Mass [kg]
1	Xe	642.78
1	Kr	49.82
2	Cs	367.74
2	Rb	46.78
3	Ba	181.08
3	Sr	124.13
5	Te	56.66
6	Ru	277.20
8	Ce	345.71
8	Zr	469.80
8	Np	56.99
8	Pu	1066.68
9	La	157.07
9	Y	64.78
9	Pr	140.83
9	Nd	477.72
9	Sm	89.28
16	CsI	27.88

Table 3.4 NUREG-1465 Source term

		Fraction of the initial core inventory	
		Gap release	Early in-vessel
Duration [hr]		0.5	1.5
Noble gases	(Xe,Kr)	0.05	0.95
Halogens	(I)	0.05	0.25
Alkali metals	(Cs,Rb)	0.05	0.20
Tellurium group	(Te)	0.0	0.05
Barium, Strontium	(Ba,Sr)	0.0	0.02
Noble metals	(Ru)	0.0	0.0025
Cerium group	(Ce,Zr,Np,Pu)	0.0	0.0005
Lanthanides	(La,Y,Pr,Nd,Sm)	0.0	0.0002

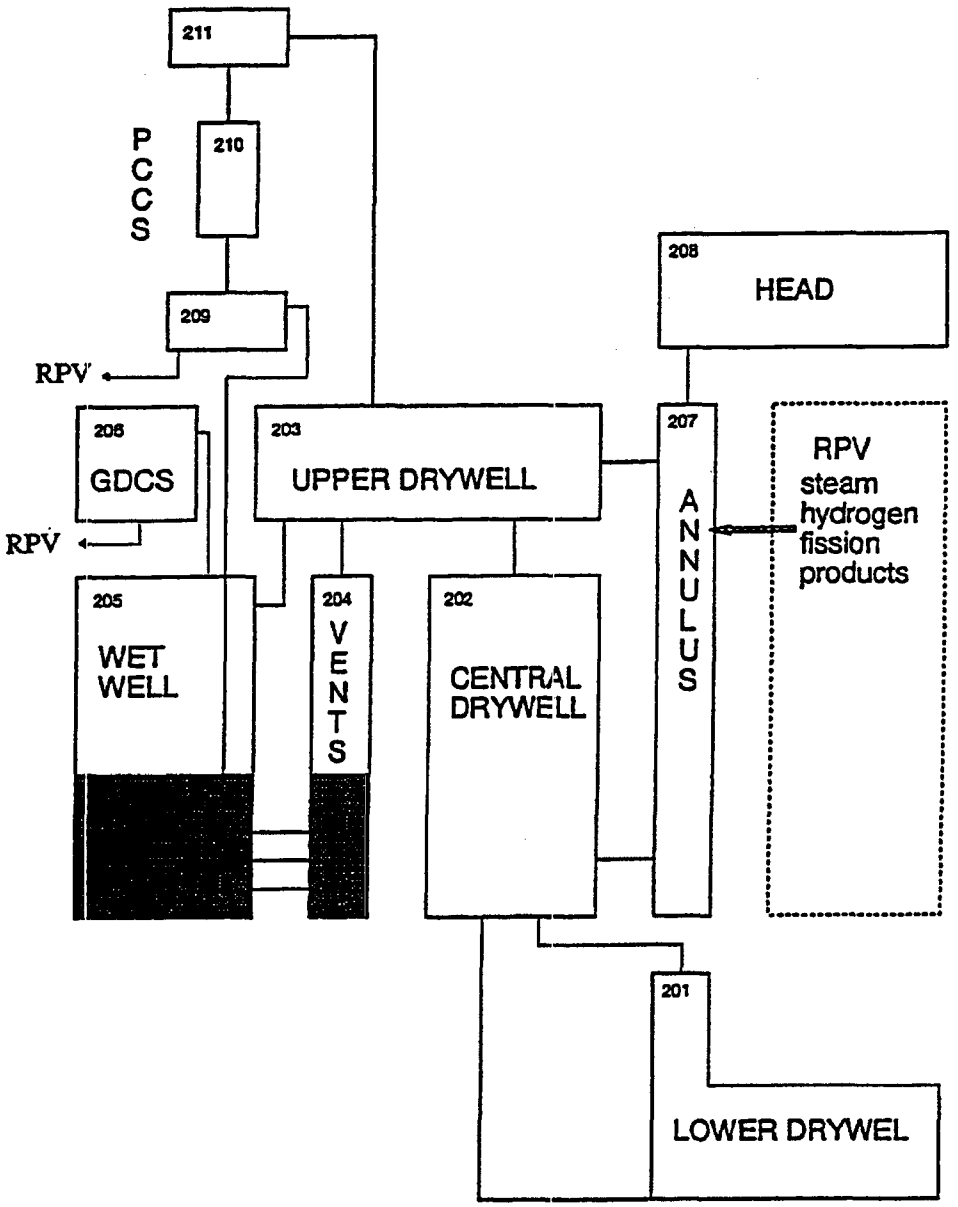

Figure 3.1 MELCOR nodalization scheme of the ESBWR containment

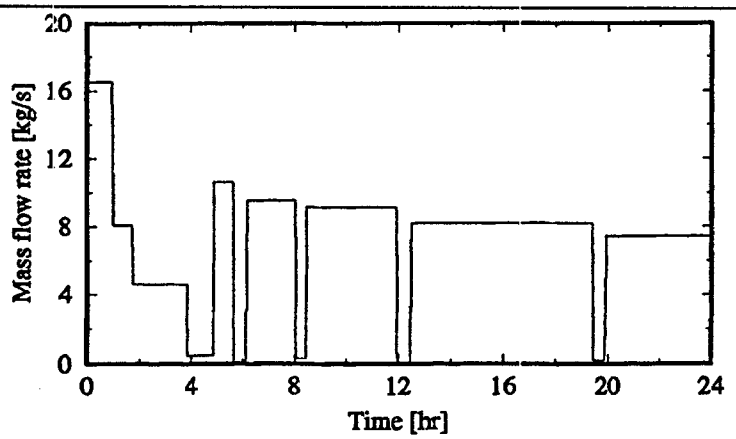

Figure 3.2 Mass flow steam from RPV

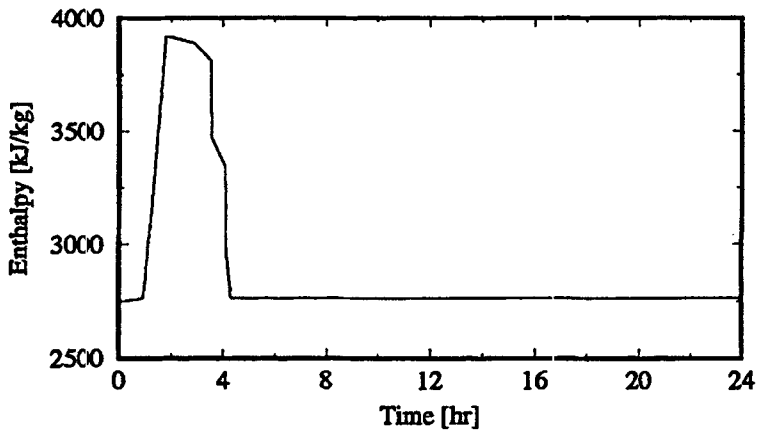

Figure 3.3 Enthalpy of steam from RPV

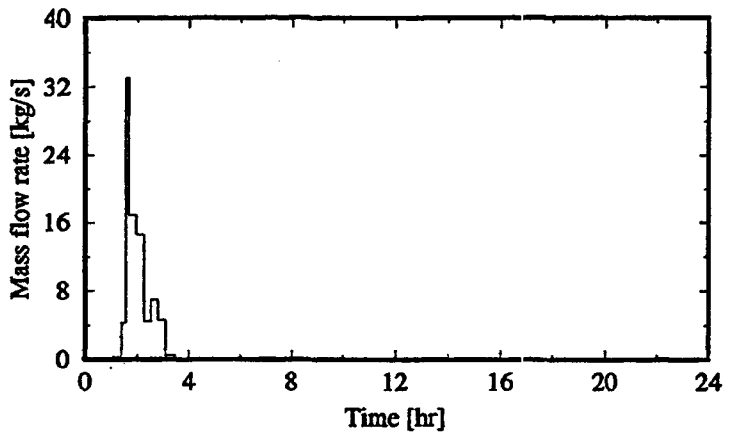

Figure 3.4 Mass flow hydrogen from RPV

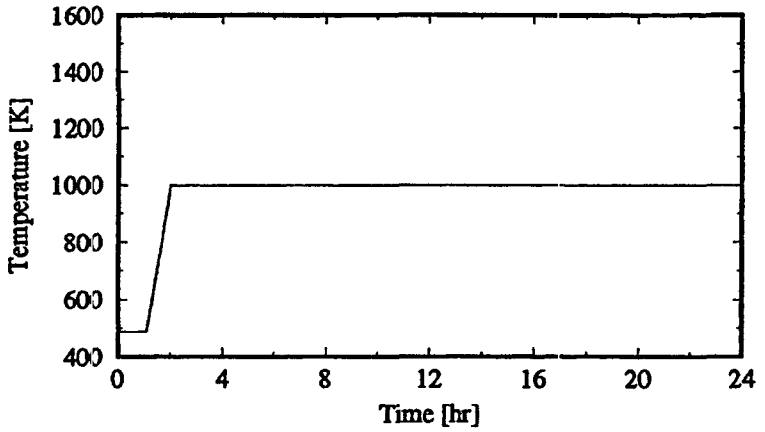

Figure 3.5 Temperature of hydrogen from RPV

4. Analysis Results

This chapter contains the results of the MELCOR analysis.

4.1 Thermal-Hydraulic Results

The pressure in the drywell increases to 0.38 MPa at about 3.5 hours due to the injection of steam and hydrogen, as can be observed from Figure 4.1. After 3.5 hours the GDCS starts draining. As a consequence, the wetwell volume increases resulting in a lower wetwell pressure and therewith a lower pressure in the upper drywell. After 4 hours, the hydrogen flow stops and the steam flow out of the RPV decreases from 4.6 kg/s to 0.45 kg/s for a period of approximately 1 hour, see Figure 3.2. Hereafter the drywell pressure decreases due to steam condensation inside the PCCS and on the drywell structures. Due to ongoing condensation on the drywell structures, the pressure in the drywell drops below the wetwell pressure. As a result, the PCCS stops working and the vacuum breakers open. As a consequence, the wetwell pressure will follow the drywell pressure. At about 5 hours, steam is injected again, the drywell pressure increases, the vacuum breakers close, and the PCCS starts working again. This sequence of steam flow reduction followed by a sharp decrease of the drywell pressure and subsequent opening of the vacuum breakers occurs four more times during the first 24 hours of this analysis, as can be observed from Figures 4.1 through 4.3. After 24 hours the drywell pressure has reached a value of 0.35 MPa and is still slowly increasing.

The gas temperatures inside the drywell, the PCCS, and the wetwell are shown in Figure 4.2. The drywell temperature has reached a value of 412 K at the end of the analysis. The wetwell gas temperature increases only 5 K from 316 K till 321 K. Since the PCCS is cooled by the IC pool, the temperature inside the PCCS decreases till the temperature of the IC pool every time the steam flow into the containment and therewith to the PCCS stops. Since the water in the IC pool increases in temperature from 300 K till 363 K at 24 hours, the temperature decrease in the PCCS becomes smaller every time.

Figure 4.3 shows the steam fraction inside the upper drywell and in the lower header of the PCCS. As long as a significant fraction of non-condensables is present in the drywell, the PCCS performance is poor. The presence of noncondensables hinders the condensation process. The moment that almost all the non-condensables are vented to the wetwell, the performance of the

PCCS increases. The steam fraction in the drywell decreases every time when the drywell pressure drops below the wetwell pressure because the vacuum breakers open and non-condensables flow from the wetwell into the drywell. When the steam flow increases, the steam fractions in the drywell and PCCS increase again. The performance of the PCCS decreases during 24 hours due to the increasing IC pool temperature.

4.2 Fission product Behavior

Noble Gas Behavior

During the "gap release" phase (1.5 - 2.0 hr, see section 3.2), 5% of the noble gases are released into the containment, while the remaining 95% is released during the "early in-vessel release" phase (2.0 - 3.5 hr). The total injected mass of the noble gases in the containment is 692.6 kg as can be seen in Table 4.1. The mass of the noble gases inside the upper drywell is shown in Figure 4.4. During the analysis, most of the noble gases are vented to the wetwell through the PCCS vent line. After about 5.5 hr, the drywell only contains some noble gases in the periods shortly after the opening of the vacuum breakers.

The distribution of noble gases is shown in Figure 4.5. The major release from the upper drywell to the RB occurs between 1.5 and 5 hr, due to the high concentration of the noble gases in the upper drywell during this period.

Figure 4.6 shows the noble gases mass flow rate into the RB. After about 5.5 hr, the release of noble gases from the containment nearly stops, because noble gases are transported to volumes that do not leak to the RB. In the 24-hr time period, a fraction of $5.4 * 10^{-4}$ of the noble gases that are released from the RPV leaks to the RB, see also Table 4.2.

Aerosol behavior

The mass of the airborne fission product aerosols in the upper drywell is shown in Figure 4.7, and the distribution of fission product aerosols is shown in Figure 4.8. The total released mass of fission product aerosols in the containment is 122.8 kg as can be seen in Table 4.1. The major release of the fission product aerosols from the RPV takes place in the "early in-vessel release" phase (2.0 - 3.5 hr). The aerosols are transported through the containment by the gas flows. After 3.5 hr, the fission products release stops, and the aerosol concentration decreases rapidly. At 5 hr, about 85% of the injected aerosols have deposited on structures mainly by diffusiophoresis. After about 5 hr, the steam flow increases, and the major part of the remaining airborne aerosols deposit inside the PCCS. Aerosols which do not deposit in the PCCS are transported by the noncondensable gases via the PCCS vent line into the wetwell. The increase in airborne aerosol mass at about 13.5 hr is caused by evaporation of liquid films on heat structures releasing aerosols in the atmosphere.

As can be seen from Figure 4.9, the major release of aerosols from the containment to the RB occurs between 1.5 and 5 hr. After this time, the release of aerosols from the containment nearly stops, because the aerosols deposit and are transported to volumes that do not leak to the RB. The release of fission product aerosols from the RPV into the containment and the release from the containment to the RB are summarized in Table 4.1 and 4.2. Table 4.2 shows that the fraction of the core inventory that is released to the RB varies considerably for different aerosol species, due to the differences in core inventory that is released from the RPV into the containment. However, the fraction of aerosols in the containment that is released to the RB (see Figure 4.8) is almost independent of the aerosol species and equals $2.7 * 10^{-4}$ after 24 hr.

The aerodynamic mass median diameter (AMMD) and the geometric standard deviation (GSD) of the aerosols in the RB, which characterize the particle size distribution of the aerosol source from the containment, are shown in Figures 4.10 and 4.11. At the start of the aerosol release (1.5 hr), the aerosol size distribution in the upper drywell is identical to the source from the RPV: the AMMD is equal to 1.0 μm and the GSD is equal to 1.6 (see section 3.2). After 1.5 hr, the AMMD increases because the released aerosols from the containment increase due to agglomeration caused by the high aerosol concentration. This high aerosol concentration is initially caused by the fission product release, and after about 5 hr, by fog formation in the upper drywell. A high concentration of fog aerosols results in a high agglomeration rate and high AMMD's. The maximum AMMD is about $6.5 * 10^{-3}$ mm at about 17 hr. From 17 hr the AMMD slowly decreases because no more aerosols are released from the containment and the greatest aerosols in the RB deposit.

The aerosol removal coefficient λ_D is shown in Figure 4.12 and is calculated by

$$\lambda_D = \frac{1}{m_g} \frac{dm_D}{dt}$$

with: m_g = airborne aerosol mass

m_D = deposited aerosol mass

The aerosol removal coefficient λ_D depends on the deposition mechanisms active and the particle size distribution. The most important deposition mechanisms are diffusiophoresis and gravitational settling. High λ_D values are expected if both mechanisms are important, and low λ_D values are expected if only gravitational settling is important. The aerosol removal coefficient roughly follows the release rate of steam from the RPV (compare Figures 3.2 and 4.12), because the steam concentration in the drywell influences the steam condensation on structures and inside the PCCS, and therewith the aerosol deposition. After about 6 hr the calculation of the aerosol removal coefficient becomes unreliable because the aerosol concentration reaches too low values. Therefore the calculation of λ_D ends at 6 hr.

Table 4.1 Injected aerosol mass in the containment after 3.5 hr

MELCOR Class	Fission product	Mass [kg]
Noble gases		
1	Xe + Kr	692.60
Aerosols		
2	Cs + Rb	103.63
3	Ba+Sr	6.10
5	Te	2.83
6	Ru	0.69
8	Ce + Zr + Np + Pu	0.97
9	La+Y+Pr+Nd+Sm	0.19
16	CsI	8.36
Total aerosols		122.77

Table 4.2 Released aerosol mass to the reactor building after 24 hr

MELCOR Class	Fission product	Mass [kg]	Fraction of core inventory [-]
Noble gases			
1	Xe + Kr	$3.72*10^{-1}$	$537*10^{-6}$
Aerosols			
2	Cs + Rb	$2.80*10^{-2}$	$68*10^{-6}$
3	Ba + Sr	$1.79*10^{-3}$	$6*10^{-6}$
5	Te	$8.32*10^{-4}$	$15*10^{-6}$
6	Ru	$2.03*10^{-4}$	$1*10^{-6}$
8	Ce + Zr + Np + Pu	$2.85*10^{-4}$	$0.2*10^{-6}$
9	La + Y + Pr + Nd + Sm	$5.50*10^{-5}$	$0.1*10^{-6}$
16	CsI	$2.29*10^{-3}$	$82*10^{-6}$
Total aerosols		$3.35*10^{-2}$	$8*10^{-6}$

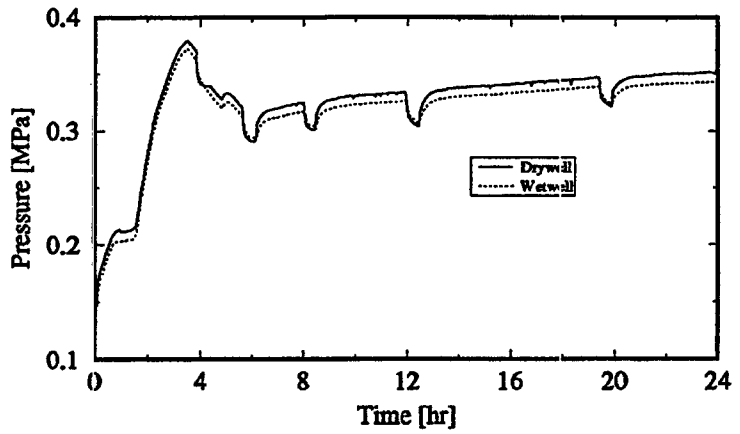

Figure 4.1 Pressure in the drywell and wetwell

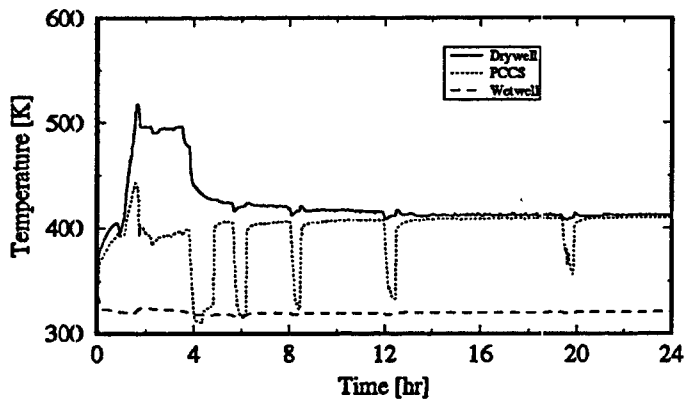

Figure 4-2 Gas temperature in the drywell, the PCCS, and the wetwell

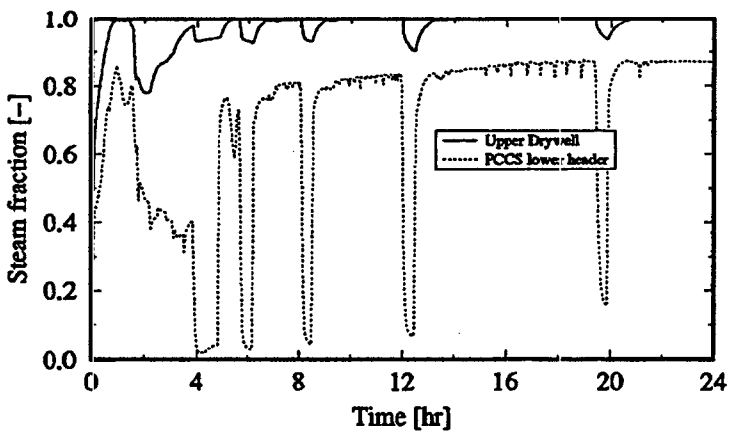

Figure 4.3 Steam fraction in upper drywell and PCCS

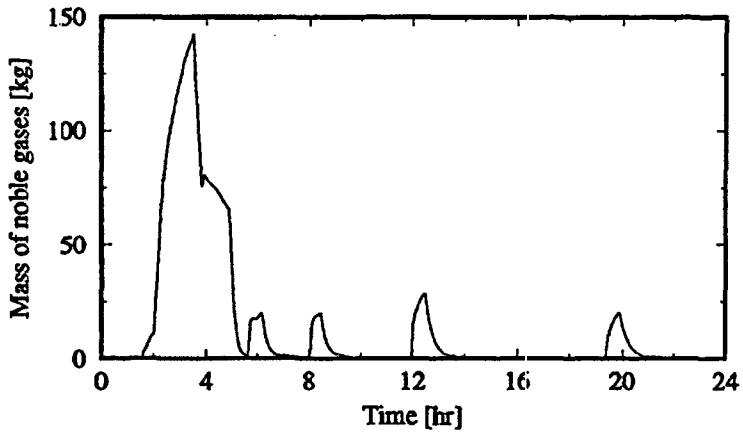

Figure 4.4 Mass of noble gases in the upper drywell

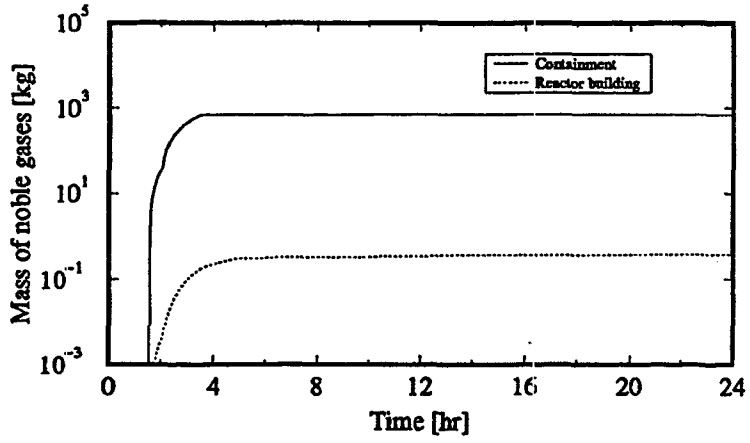

Figure 4-5 Mass distribution fo the noble gases

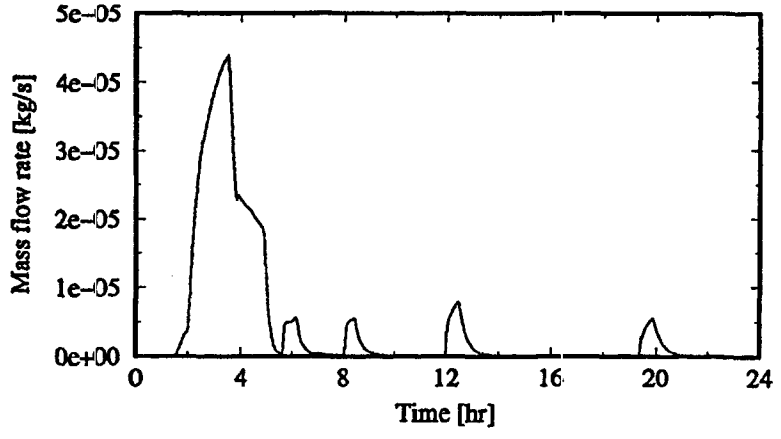

Figure 4.6 Noble gases mass flow rate in the reactor building

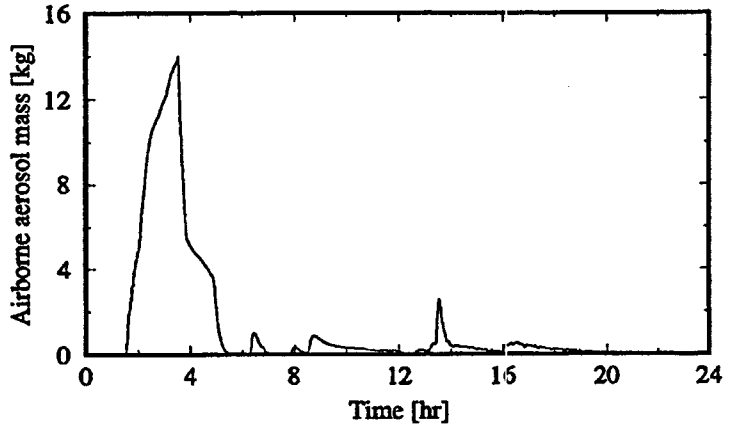

Figure 4.7 Airborne aerosol mass in the upper drywell

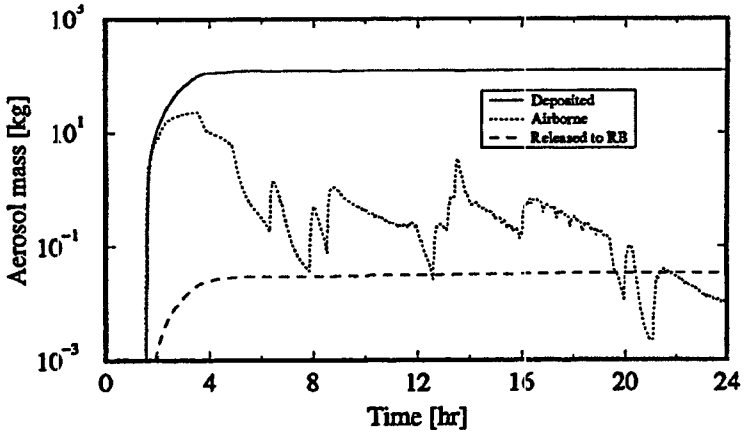

Figure 4-8 Distrbiution fo the aerosols in the containment

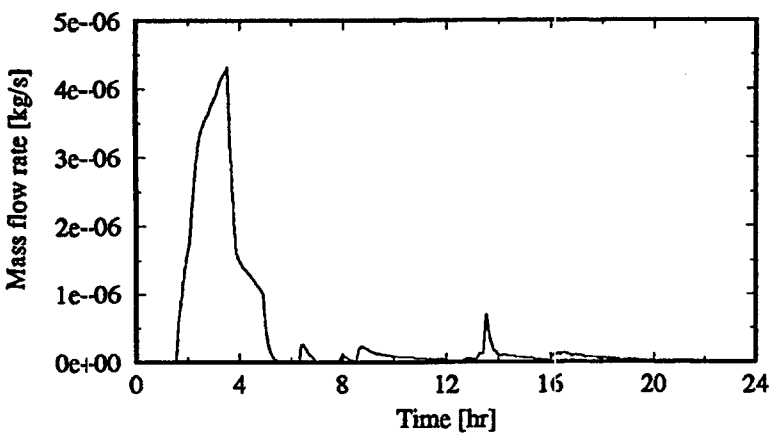

Figure 4.9 Aerosol mass flow rate into the reactor building

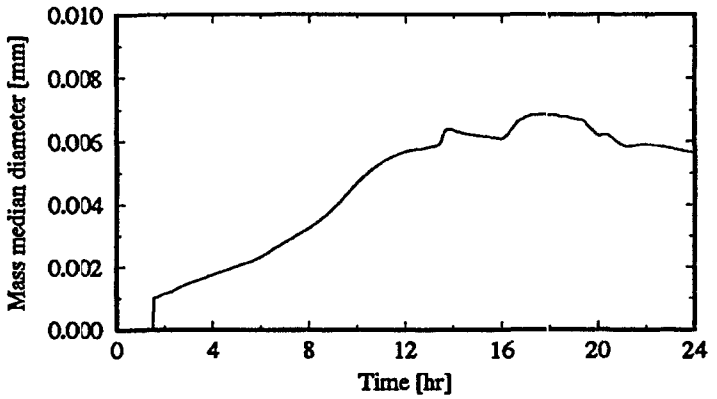

Figure 4.10 Mass median diameter of fission product aerosols in the reactor building

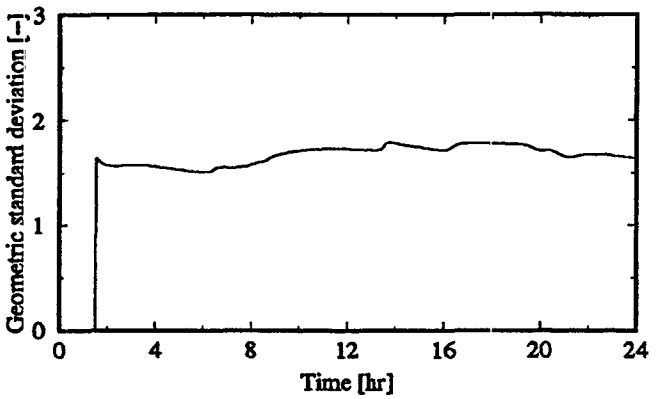

Figure 4-11 Geometric standard deviation of fission product aerosols in the reactor building

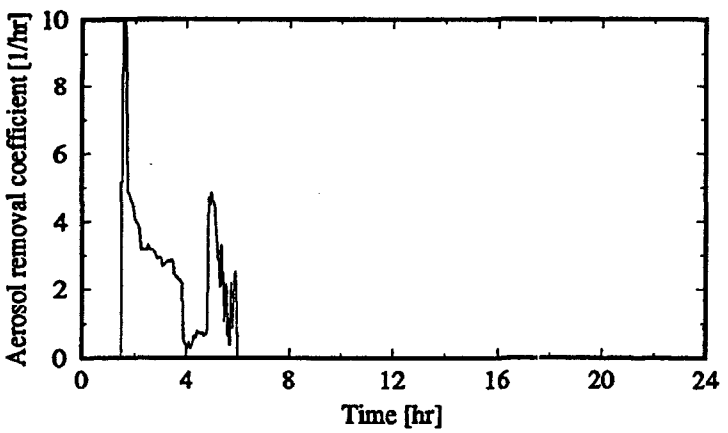

Figure 4.12 Aerosol removal coefficient λ_D in the containment

5. Conclusions

This report contains the results of an analysis which has been performed to determine the natural retention of fission products inside the ESBWR containment, using the MELCOR 1.8.3 computer code. The scenario, which was analyzed, concerned a design-basis loss-of-coolant accident. All emergency core cooling systems are assumed to fail initially. However, 2.5 hours after the water level drops below the top of the active fuel, GDCS (Gravity Driven Core Cooling System) is initiated and the molten core material is "saved" in-vessel. The containment stays intact but leaks to the RB according to the Technical Specifications. The leak rate through the penetrations is based on the design leak rate, which is 0.5 vol.%/day at a pressure of 0.483 MPa. To model the leak flow from the containment at the actual pressure, a leak area of $3.28 * 10^{-6}$ m^2 is modeled in the upper drywell region.

The masses of steam and hydrogen being released from the RPV to the containment have been calculated by GE with the MAAP code and have been used as input for the MELCOR analysis. The source term from the RPV into the containment is based on the gap release and the early in-vessel release, which are taken from NUREG-1465.

The released aerosols are deposited rapidly mainly by diffusiophoresis inside the PCCS. A small fraction is deposited on structures. The deposition rate is expressed as aerosol removal coefficient λ_D. For high steam release rates λ_D is in the order of 3/hr and for low steam release rates λ_D is about 0.5/hr.

In the 24-hr time period, a fraction of $5.4 * 10^{-4}$ of the noble gases in the containment leaks to the RB. With respect to the aerosols, the fraction of aerosols in the containment that leaks to the RB is almost independent of the aerosol species and equals $2.7*10^{-4}$ after 24 hr.

Based on the amounts of aerosols and noble gases that are still airborne after 24 hr, it can be concluded that the retention of fission products inside the containment for this scenario as calculated by MELCOR is considerable.

References

[1] Summers, R.M., et al.
MELCOR 1.8.0: A Computer Code for Nuclear Reactor Severe Accident Source Term and Risk Analyses.
SAND90-0364 (NUREG/CR-5531)
Sandia National Laboratories
Albuquerque, USA, 1991.

[2] F. Gelhard, "MAEROS User Manual", SAND80-0822 (NUREG/CR-1391), Sandia National Laboratories, Albuquerque, USA, December 1993.

13] W.R. Usry, D. McDonald, QUICK-COMM, "RPV to Drywell Info" November 18, 1993.

[4] MAAP input deck of May 1992.
SBWR Parameter File
GE Company Proprietary

[5] L. Soffer et al.: *Accident Source Terms for Light-Water Nuclear Power Plants*. Washington, DC, U.S. Nuclear Regulatory Commission. Draft NUREG-1465, June 1992.

[6] J. Hart, S. Spoelstra: Severe Accident Analyses for the SBWR, Comparison Between MAAP, MELCOR, and SCDAP/RELAP5. ECN Task 3.1, WBS 3.1.6, ECN-CX-93-012, Netherlands Energy Research Foundation ECN, Petten, The Netherlands, April 1993.

[7] S. Spoelstra, "SBWR Plant Data for MELCOR, ECN Task 3.1, WBS 3.1.6, ECN-CX-92-095, Netherlands Energy Research Foundation ECN, Petten, The Netherlands, October 1992.

List of Tables

List of Figures

List of Abbreviations

AMMD	Aerodynamic Mass Median Diameter
BWR	Boiling Water Reactor
ESBWR	European Simplified Boiling Water Reactor
GDCS	Gravity Driven Core Cooling System
GE	General Electric
GSD	Geometric Standard Deviation
IC	Isolation Condenser
IPE	Individual Plant Examination
LOCA	Loss of Coolant Accident
NRC	Nuclear Regulatory Commission
PCCS	Passive Containment Cooling System
PRA	Probabilistic Risk Assessment
PWR	Pressurized Water Reactor
RB	Reactor Building
RPV	Reactor Pressure Vessel
SBWR	Simplified Boiling Water Reactor